A Simple Empirical Model for Predicting the Decay of Tropical Cyclone Winds after Landfall

JOHN KAPLAN AND MARK DEMARIA

Hurricane Research Division, NOAA/AOML, Miami, Florida

(Manuscript received 26 January 1995, in final form 8 May 1995)

ABSTRACT

An empirical model for predicting the maximum wind of landfalling tropical cyclones is developed. The model is based upon the observation that the wind speed decay rate after landfall is proportional to the wind speed. Observations also indicate that the wind speed decays to a small, but nonzero, background wind speed. With these assumptions, the wind speed is determined from a simple two-parameter exponential decay model, which is a function of the wind speed at landfall and the time since landfall. A correction can also be added that accounts for differences between storms that move inland slowly and storms that move inland rapidly. The model parameters are determined from the National Hurricane Center best track intensities of all U.S. landfalling tropical cyclones south of 37°N for the period 1967–93. Three storms that made landfall in Florida prior to 1967 were also included in the sample. Results show that the two-parameter model explains 91% of the variance of the best track intensity changes. When the correction that accounts for variations in the distance inland is added, the model explains 93% of the variance.

This model can be used for operational forecasting of the maximum winds of landfalling tropical cyclones. It can also be used to estimate the maximum inland penetration of hurricane force winds (or any wind speed threshold) for a given initial storm intensity. The maximum winds at an inland point will occur for a storm that moves inland perpendicular to the coastline. Under this assumption, the maximum wind at a fixed point becomes a function of the wind speed at landfall and the translational speed of motion. For planning purposes, maps of the maximum inland wind speed can be prepared for various initial storm intensities and speeds of motion. The model can also be applied to the entire wind field of an individual storm to provide a two-dimensional field of the maximum wind during a given storm. Examples of each of these applications are presented.

1. Introduction

The recent landfalls of Hurricanes Hugo (1989) and Andrew (1992) have illustrated the need for more accurate predictions of the inland effects of hurricane winds. Unlike most previous U.S. landfalling hurricanes, the majority of the 36 deaths and most of the estimated \$30–\$40 billion in damage directly attributed to these storms were due to the effects of wind rather than storm surge (U.S. Department of Commerce 1993; National Research Council 1994). At the time that Hugo and Andrew made landfall, forecasters at the National Hurricane Center (NHC) relied on past experience to make inland wind forecasts since none of the operational tropical cyclone (TC) prediction models provided intensity forecasts over land. Beginning in 1992, a three-dimensional TC prediction model developed at the Geophysical Fluid Dynamics Laboratory (GFDL) provided near-real-time overwater and overland track and intensity forecasts to the NHC (Bender et al. 1993). Lawrence and Gross (1993, 1994) have shown that the GFDL model overwater track forecasts had considerable skill compared to the other tropical cyclone track models that NHC employed during the 1992 and 1993 hurricane seasons. However, their results also indicated that the GFDL overwater intensity forecasts were somewhat worse, on average, than those produced by the other intensity models. To date, no comprehensive evaluation of the GFDL overland intensity forecasts has been performed.

In contrast to the rather sophisticated GFDL model, most previous attempts to model the decay of TCs over land have been empirical. In one of the earliest such studies, Hubert (1955) found that hurricanes making landfall along the Atlantic coast of the United States filled more rapidly than those that made landfall along either the Gulf of Mexico or Florida coastlines. Malkin (1959) performed a similar study and determined that there was a tendency for the most intense hurricanes to fill the most rapidly. He also found that the filling rate of hurricanes decreased as the percentage of the storm's underlying circulation that was over water increased. More recently, Schwerdt et al. (1979) and Ho et al. (1987) showed that hurricanes making landfall

Corresponding author address: John Kaplan, AOML/NOAA, Hurricane Research Division, 4301 Rickenbacker Causeway, Miami, FL 33149.

along the Gulf of Mexico coastline filled most rapidly, while those that made landfall along the Florida coastline filled the slowest.

The primary emphasis of the above studies was the evaluation of the decrease in the pressure gradient between the TC center and the surrounding environment as a function of time since landfall. In several of these studies, some form of the gradient or cyclostrophic wind equation was used to estimate the overland maximum wind speeds consistent with these pressure gradients. Batts et al. (1980) developed a slightly more sophisticated model for determining the maximum possible inland wind speeds. In their model, the decrease in the pressure gradient after landfall was obtained using an empirical equation that was a function of the time a TC was over land and the angle at which the storm crossed the coastline. The inland wind speeds of the TC were then computed as a function of the azimuthal and radial distance from the storm center using an approximate form of the gradient wind equation. Batts et al. assumed that the translational speed of the storm resulted in an asymmetric wind field where the strongest winds were always in the right rear quadrant. Also, the inland wind speeds were reduced to account for the sudden increase in surface roughness experienced immediately after a TC makes landfall. Georgiou (1985) used a similar approach but added a level of complexity by employing a modified version of Shapiro's (1983) hurricane planetary boundary layer model to predict both inland wind speeds and directions. The decrease in the pressure gradient after landfall required to run this model was determined by an empirical relationship developed for four separate regions of the United States. Unlike most previous studies, the filling rates obtained by Georgiou were a function of distance inland rather than time inland.

In this study, a simple empirical model for predicting TC wind speeds after landfall is described. This model directly predicts the decrease in wind speeds, rather than predicting the pressure increase and then inferring the winds from the pressure. A correction term that accounts for the distance a TC is inland is included in the model. This term is used to account for storms that move at some angle to the coastline rather than perpendicular to the coast at landfall. The dataset used to develop the model is described in section 2, and the derivation of the model is discussed in section 3. Applications of the decay model are presented in section 4. Conclusions and ideas for future research are discussed in section 5.

2. Data

The database used to derive the decay model consists of all named TCs that made landfall in the United States from 1967 to 1993, and a few additional TCs that made landfall along the Florida coastline prior to 1967. Tropical cyclone position and intensity estimates for the 1967–93 cases were obtained from the HURDAT file maintained by NHC (Jarvinen et al. 1988). The lone exception is for the intensity estimates of Hurricane Andrew (1992) over Florida, which were obtained from Powell and Houston (1995, unpublished manuscript). The HURDAT file consists of 6-h estimates of position, central pressure, and maximum sustained 1-min surface wind speed (MSSW) for all named Atlantic TCs from 1886 to 1993. Landfalling TCs prior to 1967 were not used in this study because Neumann (1994) found that the HURDAT file is less reliable for pre-1967 events. The problem with these earlier events is that TC position and intensity estimates were only archived once per day before 1931 or twice per day prior to the mid-1950s. From the mid-1950s to the mid-1960s, positions and intensities were determined every 6 h, although not all of the 6-h values were saved. Consequently, interpolation was necessary to obtain the intermediate 6-h position, central pressure, and wind estimates for many TCs during the pre-1967 era. This was accomplished by employing nonlinear interpolation to estimate the intermediate 6-h positions, while a simple linear interpolation between existing intensity estimates was used to obtain the intermediate wind speeds and pressure. Neumann found that while this technique worked fairly well when a TC was over water, serious problems were detected in some overland position and intensity estimates. He indicated that the problems with overland intensity estimates were especially troublesome because a linear interpolation scheme was used to obtain intensity estimates at intermediate times even though the decay of TCs has been shown to be nonlinear (Malkin 1959; Schwerdt et al. 1979; Ho et al. 1987). The errors in the overland positions, while not as serious as those for the overland intensities, did result in some storms crossing the coastline at incorrect locations. Thus, except for a few Florida landfalling cases that were hand analyzed, only TCs that made landfall from 1967 to 1993 are used in this study.

The sample was also restricted to TCs that made landfall from near the Texas–Mexico border to the North Carolina–Virginia border. Tropical cyclones making landfall outside the United States were excluded because fewer surface observations are routinely available for the poststorm analysis in these regions. Tropical cyclones making landfall north of the North Carolina–Virginia border were not used because they likely have different decay properties than those in other regions. These differences are probably due to more frequent interactions with extratropical systems as well as the comparatively large variations in the terrain type (i.e., forest, hills, etc.) encountered after landfall. Moreover, TCs in this region are typically weakening at landfall due to the effects of the cooler surface waters at these latitudes. Consequently, the assumption made later in this paper (section 3) that TCs exhibit little change in intensity just prior to landfall is clearly not valid for this region. For these reasons, a separate study of the decay of TCs in this area is planned for the future.

Because relatively few hurricanes made landfall along the Florida coastline during the period 1967–93, it was desirable to include a few hurricanes that made landfall in this area prior to 1967. This is particularly important for evaluating the claim of previous authors (Malkin 1959; Schwerdt et al. 1979; Ho et al. 1987) that TCs making landfall along the Florida coastline fill less rapidly than TCs in other regions in the United States (e.g., Gulf Coast). As discussed above, the HURDAT file is less accurate prior to 1967. Therefore, surface data archived at the National Climatic Data Center (NCDC) in Asheville, North Carolina, were employed to aid in determining TC position and intensities for Hurricanes Donna (1960) and Cleo (1964). Wind data were also obtained for the unnamed 1949 Florida hurricane from a study by the U.S. Weather Bureau (1951). These storms were chosen because of the availability of surface observing stations along the path of these hurricanes. Details of the procedures used to obtain MSSW estimates for these Florida hurricanes are contained in the appendix.

The MSSW estimates that were obtained for the three Florida hurricanes by the procedures described in the appendix were, on average, approximately 20 kt lower than those in the HURDAT file. Since previous studies (i.e., Powell et al. 1991) indicate that wind speeds just a few kilometers inland are only about 80% as large as the winds on the coast, the higher wind speed values in the HURDAT file could, in part, be the result of estimating inland wind speeds by interpolating between the higher wind speeds observed on the east and west coasts of Florida. Whatever the reason for these differences, it is believed that the intensity estimates for the landfalling Florida hurricanes used in this study, while not perfect, are comparable in accuracy to those found in the HURDAT file commencing in 1967.

The tracks of the three landfalling Florida hurricanes as well as the other 64 landfalling TCs used to derive the decay model are depicted in Fig. 1. The sample includes 401 MSSW estimates (at 6-h intervals) from these 67 TCs. Nearly all of these TCs dissipated, became extratropical, or moved back over water within 48 h. The average postlandfall duration of each TC was 17 h, and the average decrease in the MSSW was 28 kt. In this paper, knots are used instead of meters per second because the MSSW values in the HURDAT file are specified in 5-kt increments. More important, this decision was made because the decay model is being developed for operational use by the NHC and the Federal Emergency Management Agency, both of whom provide wind forecasts and warnings in units of knots.

3. Model development

Previous observational (Miller 1964) and numerical modeling studies (Ooyama 1969; Rosenthal 1971; Tuleya et al. 1984) have shown that the primary mechanism responsible for the rapid decay of TCs after landfall is the greatly reduced latent and sensible heat fluxes over land. More recently, Tuleya (1994) demonstrated that the reductions in these fluxes were due to the decreased land temperature beneath the storm center. This reduction in surface land temperature was a result of the finite heat capacity and conductivity of the soil subsurface. The above modeling studies, as well as observational studies performed by Schwerdt et al. (1979) and Ho et al. (1987), have also shown that the rate of decay of TCs is largest just after landfall and that the decay rate is proportional to the landfall intensity.

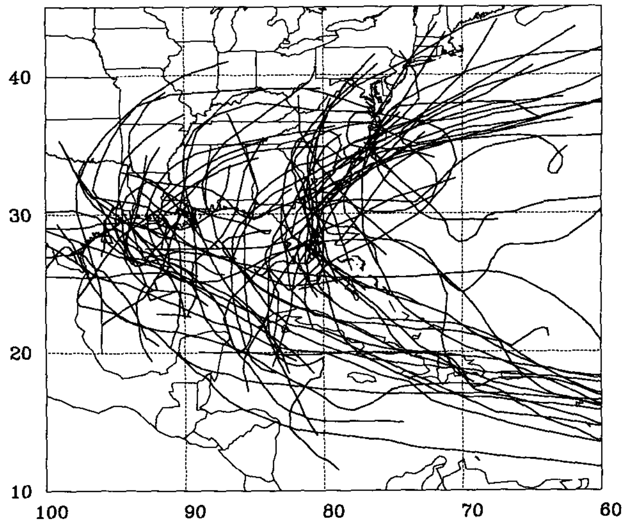

FIG. 1. Tracks of the 67 landfalling TCs used to develop the decay model.

The availability of the relatively large database obtained for the current study makes it possible to evaluate these findings by examining the decrease in the MSSW of all landfalling TCs in this data sample. In this study, the landfall intensity was assumed to be the MSSW at the time the TC crossed the coastline. Since the HURDAT file does not contain either the time or the intensity of the TC at landfall, it was necessary to estimate this information from the available data. The time of TC landfall was obtained by linearly interpolating the HURDAT positions to the landfall point. The intensity at landfall was assumed to be the MSSW at the time closest to but proceeding landfall. Thus, since the HURDAT file has 6-h resolution, this MSSW could be representative of the storm intensity up to 6 h prior to TC landfall. While these procedures could introduce some uncertainty, Merrill (1987) found that the median 12-h intensity change for Atlantic TCs within about 200 km of the coastline was nearly zero. Therefore, while the MSSW values at landfall may be inaccurate for some TCs, they should be reasonable for the majority of the cases employed in this study.

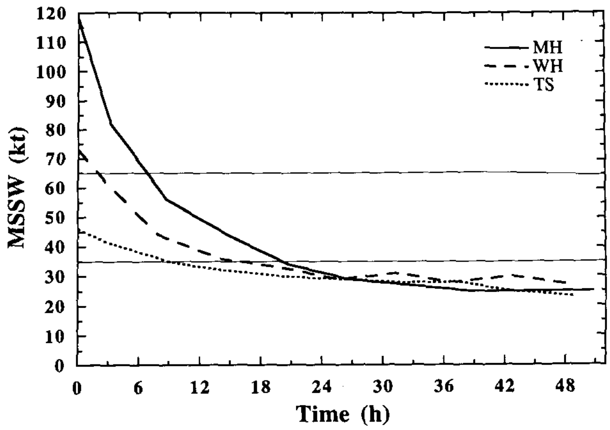

FIG. 2. The mean change in MSSW as a function of the elapsed time after landfall for the mean tropical storm (TS), weak hurricane (WH), and major hurricane (MH). The solid horizontal lines depict the threshold of hurricane- (65 kt) and tropical-storm- (35 kt) force MSSWs.

To illustrate the effect of initial intensity on decay rate, all TCs were placed into one of three stratifications—tropical storm ($35 \leqslant$ MSSW $\leqslant 63$), weak hurricane ($64 \leqslant$ MSSW $\leqslant 96$), and major hurricane (MSSW $\geqslant 97$)—based on their MSSW (kt) at landfall. Figure 2 shows the average intensity of each of these stratifications as a function of the elapsed time after landfall. This figure indicates that although the rate of decay of the MSSW of major hurricanes exceeds the decay rate for both weak hurricanes and tropical storms, the shapes of the decay curves are quite similar. Figure 2 also suggests that TCs decay to approximately the same MSSW after about 24–30 h regardless of their intensity at landfall. It is interesting to note that even the average major hurricane falls below hurricane intensity in about 7 h and below tropical storm strength in about 20 h.

a. Derivation of the decay model

The assumption that TCs decay at a rate that is proportional to their landfall intensity is the basis of our empirical inland wind decay model (IWDM) and can be expressed by the following differential equation:

$$\frac{dV}{dt} = -\alpha V, \tag{1}$$

where V (kt) is the MSSW, α is the decay constant (h^{-1}), and t (h) is the time after landfall. The solution to (1) is given by

$$V(t) = V_0 e^{-\alpha t}, \tag{2}$$

where V_0 is the MSSW at $t = 0$.

As shown in Fig. 2, the MSSW decays to some background wind speed V_b. This effect can be included by adding an extra term to (1) to give

$$\frac{dV}{dt} = -\alpha(V - V_b), \tag{3}$$

which has a solution given by

$$V(t) = V_b + (V_0 - V_b)e^{-\alpha t}. \tag{4}$$

The observational results of Myers (1954), Schwerdt et al. (1979), Powell (1982, 1987), and Powell et al. (1991) indicate that hurricane winds decrease abruptly as the landfalling storm crosses the coastline. Powell et al. (1991) noted that this rapid decrease in wind speed occurs within a few kilometers of the coastline as onshore winds quickly adjust to the increased roughness of the underlying land surface. Consequently, V_0 in (4) is multiplied by a reduction factor R to account for this rapid decrease to give

$$V(t) = V_b + (RV_0 - V_b)e^{-\alpha t}. \tag{5}$$

The parameters V_b and α in (5) were determined by minimizing the error between the predicted and observed values of V using the method of least squares for a range of R values. Table 1 indicates that the variance explained r^2 by the IWDM generally exceeds 90%. The relatively high r^2 values in the table demonstrate that the model does a good job of reproducing the decay rate of the landfalling cases. A slightly better fit was obtained with $R = 1.0$ or 0.9 than with 0.8 or 0.7. The slight increase in the mean absolute error (AE) and the root-mean-square error (rmse) with $R = 0.8$ or 0.7 resulted from underestimation of the MSSW for data points within 12 h of landfall. Table 1 also shows that the magnitude of α decreases as R decreases, but the magnitude of V_b is nearly the same for all R values. The relatively constant V_b value is consistent with Fig. 2, which shows that after landfall TCs decay to the same MSSW regardless of their initial intensity.

b. Correction for proximity to the coastline

The results of Malkin (1959) suggest that TCs whose circulations are partially over water decay less rapidly than those that are entirely over land. This result seems reasonable since a TC that remained partially over water would presumably experience larger fluxes of heat and moisture than a TC entirely over land. To determine if such a mechanism could be observed in the

TABLE 1. The variance explained r^2, mean absolute error AE, root-mean-square error rmse, and α and V_b coefficients obtained for a series of R values used in the IWDM.

R	r^2 (%)	AE (kt)	rmse (kt)	α (h^{-1})	V_b (kt)
1.0	91	6.4	8.8	0.115	27.0
0.9	91	6.5	8.8	0.095	26.7
0.8	91	7.0	9.2	0.080	26.9
0.7	89	8.0	10.4	0.069	28.0

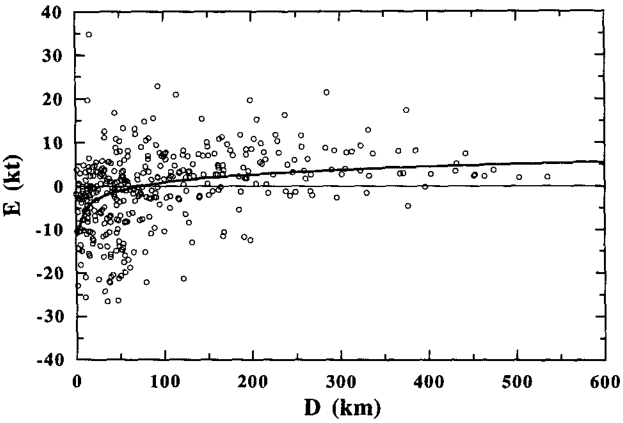

FIG. 3. The relationships between the IWDM error E and the mean distance inland D of a TC during the forecast period. The best-fit line for these points is also shown.

current dataset, the average distance inland D was calculated for each observation. Figure 3 is a scatter diagram where the y axis is the error E between the MSSW predicted using (5) (assuming $R = 0.9$) and the observed MSSW, and the x axis is D. Also shown in Fig. 3 is the best-fit line for these points. A logarithmic relationship was employed rather than a linear relationship because of the superior fit obtained when using such a technique.

Although the data points exhibit considerable scatter, Fig. 3 suggests that on average the IWDM tends to underpredict ($E < 0$) the MSSW of landfalling TCs closest to the coastline while overpredicting ($E > 0$) the MSSW of TCs farther inland. However, Fig. 3 also indicates that the average model bias is fairly small ($E \leqslant \sim 5$ kt), except very near the coastline where a more significant negative bias is evident. This negative bias suggests that storms nearer to the coastline decay less rapidly than those farther inland as suggested by Malkin (1959). Shea and Gray (1973) and Samsury and Zipser (1995) found that the mean radius of maximum wind of hurricanes is approximately 35 km. Moreover, Jorgensen (1984) and Black et al. (1995, unpublished manuscript) determined that the mean width of the eyewall of hurricanes is about 20–25 km. The results of Jorgensen (1984) also indicate that on average slightly more than 50% of the eyewall convection lies beyond the radius of maximum wind. These results indicate that, on average, the eyewall convection surrounding the mean TC extends 50 km from the TC center. Figure 3 indicates that on average the IWDM predicts too much decay for TCs with $D \leqslant 70$ km. This result is consistent with the above inner-core studies and suggests that when $D \leqslant 70$ the eyewall of many TCs remains partially over water, resulting in less decay than is observed for TCs for which D exceeds 70 km.

To include the effect of the distance inland, a correction term C was added to (5) to give

$$V(t) = V_b + (RV_0 - V_b)e^{-\alpha t} - C, \tag{6}$$

where C is expressed by

$$C = m\left[\ln\left(\frac{D}{D_0}\right)\right] + b \tag{7}$$

and D is restricted using $D \geqslant 1$. In (7), D is specified in units of kilometers, $D_0 = 1$ km, and the slope m and intercept b are constants determined by a least squares fit. Inspection of the size of the AE with time indicates that smaller model errors result when the values of m and b in (7) are allowed to vary with time. Figure 4 shows the values of m and b obtained for forecasts grouped in 6-h forecast periods assuming $R = 0.9$. Best-fit curves for m and b as quadratic functions of time are also shown in Fig. 4. These best-fit curves are used to determine m and b in (7) to obtain forecasts of $V(t)$, which are continuous in time. The best-fit curves for m and b for the $R = 0.9$ case are given by

$$m = c_1 t(t_0 - t) \tag{8}$$

and

$$b = d_1 t(t_0 - t), \tag{9}$$

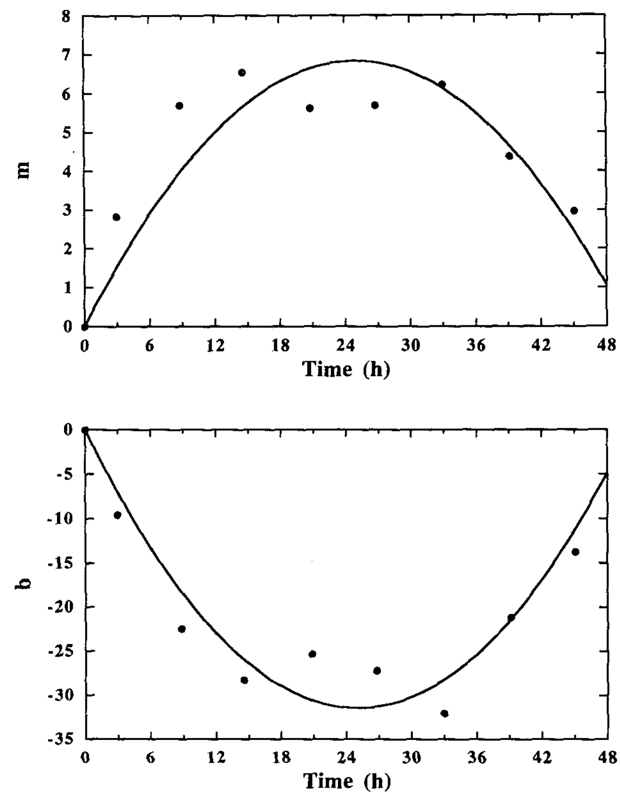

FIG. 4. The variation of the slope m (top) and intercept b (bottom) of the correction term employed in the IWDM as a function of forecast time. The quadratic best-fit lines for these points are also shown.

TABLE 2. As in Table 1 except for the version of the IWDM that includes a correction term that accounts for the mean distance inland D of a TC during the forecast period. The results from Table 1 are shown in parentheses to facilitate comparison between the two versions of the IWDM.

R	r^2 (%)	AE (kt)	rmse (kt)	α (h^{-1})	V_b (kt)
1.0	92 (91)	6.4 (6.4)	8.4 (8.8)	0.115 (0.115)	27.0 (27.0)
0.9	93 (91)	6.2 (6.5)	8.0 (8.8)	0.095 (0.095)	26.7 (26.7)
0.8	93 (91)	6.3 (7.0)	8.1 (9.2)	0.080 (0.080)	26.9 (26.9)
0.7	91 (89)	6.8 (8.0)	8.8 (10.4)	0.069 (0.069)	28.0 (28.0)

where $c_1 = 0.0109$ kt h^{-2}, $d_1 = -0.0503$ kt h^{-2}, and $t_0 = 50$ h.

Table 2 shows the error statistics for the IWDM using the values of C obtained from (7). This table indicates that the use of the correction term results in an increase in r^2 of about 1%–3% depending upon which R value was employed in the model. The table also shows that the size of the AE and the rmse are reduced by approximately 0%–15% and 5%–15%, respectively, when the correction term is included. While these improvements are not particularly large, they do suggest that correcting for the distance inland of a TC during the forecast period adds some skill to the the basic version of the IWDM model. No changes are observed in the values of α and V_b since the correction term simply fits the residual error of the basic decay model.

The results in Table 2 indicate that the use of an R of 0.9 yields the smallest errors (AE and rmse) for the case when the correction term is included in the IWDM model. More importantly, most of the improvement was for cases within the first 12 h after landfall (not shown). This is significant since Fig. 2 indicates that most TC decay occurs within this first 12 h. Although Table 2 shows that the use of $R = 0.8$ yielded nearly as good a prediction, it was decided that a conservative approach should be taken, and consequently the larger R value of 0.9 was employed in the model.

Equation (10) shows the final version of the IWDM used in the remainder of this paper:

$$V(t) = V_b + (RV_0 - V_b)e^{-\alpha t} - C, \qquad (10)$$

where $R = 0.9$, $V_b = 26.7$ kt, and $\alpha = 0.095$ h^{-1}. If included, the correction factor C is given by (7) with m and b determined from (8) and (9).

Figure 5 shows a scatter diagram of the observed versus model-predicted changes in MSSW. This figure indicates that there is generally good agreement between the predicted and observed changes although the model does not perform quite as well during the first 12 h after landfall as it does for for predictions made for $t \geq 12$ h. The increased difficulty in the first 12 h is likely due to the uncertainty both in the time of TC landfall and in the landfall intensity.

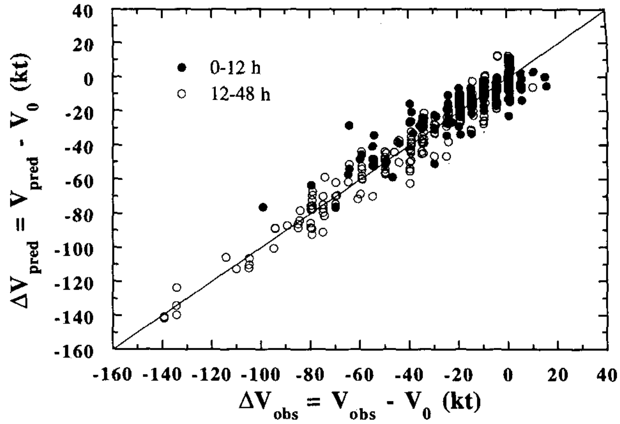

FIG. 5. The observed ($\Delta V_{obs} = V_{obs} - V_0$) versus the model-predicted ($\Delta V_{pred} = V_{pred} - V_0$) change in MSSW for the 401 landfall cases used to develop the IWDM. The solid circles denote forecasts made within the first 12 h after landfall, while the open circles indicate forecasts for the period from 12 to 48 h after landfall.

c. Regional variations in decay rates

As discussed in section 1, several previous studies (e.g., Schwerdt et al. 1979; Ho et al. 1987) have suggested that there are regional differences in the decay rates of landfalling TCs. To investigate whether such differences could be detected in the current dataset, the U.S. coastline was divided into three geographical regions (Gulf Coast, East Coast, and Florida) as shown in Fig. 6. These regions were chosen for consistency with previous studies. Four versions of the model will be compared. The first version is the same as the one described previously, using all 401 landfalling TC cases [i.e., Eq. (10)]. This version will be referred to as the USIWDM in the remainder of this section. The other

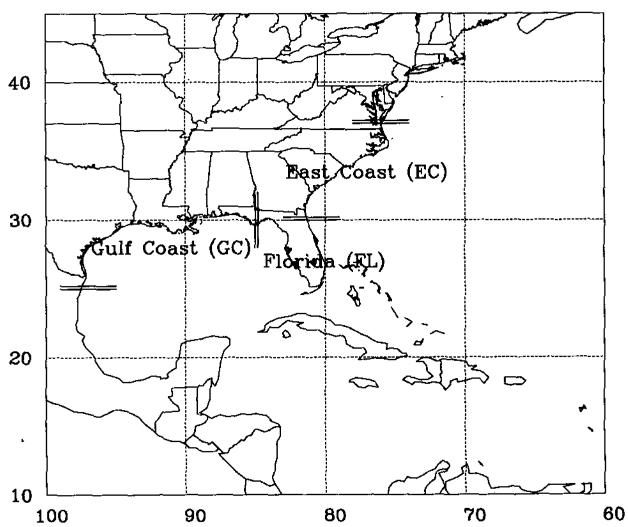

FIG. 6. The three different geographic regions (Gulf Coast, East Coast, and Florida) for which the IWDM was derived.

three versions of the model were obtained by rederiving the model (new values of α, V_b, and the correction term coefficients were computed) separately for each region employing only those TCs that made landfall in that particular region. These new versions of the model are referred to as the GCIWDM, ECIWDM, and FLIWDM for the Gulf Coast, East Coast, and Florida region, respectively. An R value of 0.9 was employed in all versions of the model since this value yielded the smallest model errors for all regions.

The results for the three regional versions of the model are shown in Table 3. The errors obtained without the correction term (not shown) were similar to, although somewhat larger than, those in Table 3. The results in Table 3 indicate that the AE and rmse obtained using the GCIWDM and ECIWDM models are only a few percent smaller than those obtained using the USIWDM. Moreover, there is no significant improvement in r^2 in these two regional models, relative to the USIWDM. This lack of improvement is true even though the α values differ by 9%–27% for the Gulf Coast and East Coast regions, respectively. Unlike the results obtained for the other two regions, Table 3 indicates that the use of the regional Florida model (FLIWDM) did not result in improvement over the USIWDM. This lack of improvement is due to the difficulties encountered when evaluating the correction term used in the FLIWDM. For reasons described in succeeding paragraphs, the relatively small number of cases combined with the low average MSSW of the Florida landfalling sample made accurate evaluation of the correction term more difficult for Florida than it was for the other two regions.

The differences in the error statistics of the regional versions of the IWDM relative to the USIWDM are smaller than might be expected given the magnitude of the differences in α and V_b. This result is due to the more significant improvement in model performance that occurs when the correction term is included in the USIWDM, relative to the regional models. The smaller number of landfall cases in the regional samples increased the noise in the estimates of m and b for each 6-h forecast interval. This noise made it more difficult to fit the quadratic time variation, as shown in Fig. 4 for the total sample.

Although Table 3 suggests that α varies from region to region, it is unclear whether these variations are due to actual differences in the meteorological conditions or are the result of other nonmeteorological factors. One possible nonmeteorological factor is the effect of data errors on the estimation of α. To see this effect, consider (10) without the small correction term C. If $RV_0 - V_b$ is small relative to V_b (weak storms at landfall), α can be varied significantly without much change in $V(t)$. This result indicates that when α is estimated using observations, small errors in $V(t)$ will lead to large errors in α. Conversely, if $RV_0 - V_b$ is large relative to V_b (strong storms at landfall), α cannot be varied very much without significantly affecting $V(t)$. Therefore, when estimating α from observations, small errors in $V(t)$ will not lead to large errors in α, relative to the case when $RV_0 - V_b$ is small. To illustrate this principle, first assume that (10) is exactly valid for the case with $C = 0$. Then, consider a storm with a landfall intensity of 41 kt (the average for the Florida sample in Table 3). After 6 h, the intensity will be reduced to 32.5 kt. Now, suppose there was a 5-kt error in the intensity estimate at 6 h ($V = 37.5$ or 27.5 kt), and these values were used to estimate α. If these values of V are substituted into (10) and it is assumed that V_b is fixed (since V_b in Table 3 did not vary very much from region to region), (10) can be solved for α yielding α values of -0.010 and 0.424 h^{-1} when $V = 37.5$ and $V = 27.5$ kt, respectively. If the initial intensity of a storm at landfall was 72 kt (the average for the Gulf Coast sample), then the intensity at 6 h from (10) would be 48.2 kt. A 5-kt error at 6 h would imply $V = 53.2$ or 43.2 kt, which gives α values of 0.061 or 0.140 h^{-1}. Thus, for a 5-kt error in V at 6 h, α would range from -0.010 to 0.424 h^{-1} when $V_0 = 41$ kt, compared with a range of only 0.061–0.140 h^{-1} when $V_0 = 72$ kt.

The above discussion indicates that the uncertainty in the estimate of α is greater for the case when the landfall intensity of the storm is lower. The smaller values of α in Table 3 for the Florida cases might then be due to this effect since the average landfall intensity

TABLE 3. IWDM statistics for the three separate geographic regions (i.e., Gulf Coast, East Coast, and Florida). Statistics are also presented for the USIWDM applied to the regional model samples. The results shown are for the version of the IWDM that corrects for the mean distance inland D of a TC during the forecast period and that employs a reduction factor R of 0.9. The number of cases N, the mean landfall MSSW $\overline{V_0}$, the average forecast duration $\bar{T}$, and the mean change in MSSW during the forecast period $\overline{\Delta V}$ are also shown for each region.

Region	Model version	r^2 (%)	AE (kt)	rmse (kt)	α (h^{-1})	V_b (kt)	N	$\overline{V_0}$ (kt)	$\bar{T}$ (h)	$\overline{\Delta V}$ (kt)
Gulf Coast	GCIWDM	94	5.6	7.7	0.104	25.5	246	72	19.1	37.5
	USIWDM	94	5.8	7.8	0.095	26.7				
East Coast	ECIWDM	78	6.2	7.7	0.069	28.5	68	58	15.7	19.5
	USIWDM	76	6.6	8.1	0.095	26.7				
Florida	FLIWDM	39	7.4	9.1	0.038	30.0	87	41	13.8	5.8
	USIWDM	46	7.1	8.6	0.095	26.7				

was less than in other regions. Of course, α was not determined from a single observation but was estimated by a least squares fit to multiple observations. However, if the intensity estimates were biased, the same analysis would apply. A small positive bias in the estimates of the storm intensity after landfall, or negative bias in the intensity estimate at landfall, could account for the low value of α in Table 3 for the Florida sample. Also, since the effect of this bias is less for stronger storms, the estimate of α might be expected to increase as the average intensity increases. This increase can be seen in Table 3 where $\alpha = 0.038$, 0.069, and 0.104 for the Florida, East Coast, and Gulf Coast samples, which have average landfall intensities of 41, 58, and 72 kt, respectively.

The above results suggest that the regional differences in the decay model can be accounted for by differences in the landfall intensities combined with a small intensity bias and so are not considered reliable. Therefore, the USIWDM [Eq. (10)] developed with the total sample should be used in all three regions. The lack of strong regional differences in the storm decay rate is consistent with the modeling study of Tuleya (1994), which shows that TC decay after landfall results from the significant reduction in sensible and latent heat fluxes due to the reduced land temperature beneath the storm. This reduction in land temperature is due to the low heat capacity and conductivity of the soil subsurface. Although the heat capacity and conductivity have regional variations, these variations are small relative to ocean–land differences.

The rejection of the regional differences in the decay rate in Table 3 contradicts results from previous studies. Schwerdt et al. (1979) and Ho et al. (1987) indicated that the decay rate (as measured by minimum sea level pressure deficit) is largest for Gulf storms, slightly smaller for East Coast storms, and much smaller for Florida storms. However, similar to the results in Table 3, the Gulf Coast sample in these two studies contained the most intense storms. Thus, small biases in the intensity estimates may have contributed to regional differences in their decay rates. In addition, the Florida sample in these two studies included only four hurricanes, where the data for three of these storms were obtained from Malkin (1959). The main weakness of the Malkin study was the uncertainty in the pressure at landfall. The absence of aircraft reconnaissance data made it necessary for Malkin to rely primarily on pressure observations collected at the synoptic map times when computing the filling rate for each of these hurricanes. These synoptic maps were available every 3 h for the latter two hurricanes but only every 12 h for the earliest one. Moreover, since these hurricanes did not make landfall at precisely the synoptic map times, Malkin was forced to estimate the landfall pressures of these hurricanes by various means, including interpolating backward in time using the decay rate observed at the first available synoptic time. Since previous studies have shown that the rate of decay of TCs decreases with increasing time after landfall, the decay rate that was applied backward in time was probably too small. The use of such a technique would likely yield a landfall pressure that was too high, resulting in underestimation of the decay rate computed for these hurricanes.

Further support for the hypothesis that the decay rates for Florida cited by Schwerdt et al. (1979) and Ho et al. (1987) are too low can be found in the recent landfall of Hurricane Andrew (1992). Mayfield et al. (1994), using aircraft reconnaissance observations as well as numerous surface observations, determined that Andrew made landfall just south of Miami, with a central pressure of approximately 922 mb and exited the west coast of Florida with a pressure of 951 mb. By the procedures outlined in section 2, Andrew required about 3.2 h to traverse the Florida peninsula. Following the methodology of Ho et al. (1987), it is possible to compute the filling rate FR using

$$\mathrm{FR} = \frac{\Delta P_t}{\Delta P_0}, \tag{11}$$

where ΔP_0 is the pressure deficit at the time of landfall and ΔP_t is the pressure deficit at some time t after landfall. The pressure deficit after landfall ΔP_t is defined by:

$$\Delta P_t = P_n - P_t, \tag{12}$$

where P_n is the mean pressure around a TC and P_t is the central pressure of the TC at some specified time t after landfall. Both of these quantities are specified in units of millibars.

Ho et al. (1987) used a climatological value of 1013 mb for P_n. Substituting $P_n = 1013$ mb and $P_0 = 922$ mb (Andrew's landfall pressure) into (12) yields $\Delta P_0 = 91$ mb. Following the same procedures yields $\Delta P_{3.2} = 62$ mb. From (11), the observed FR for Andrew at $t = 3.2$ h is then 0.68. This observed FR can be compared with the results of Schwerdt et al. (1979) and Ho et al. (1987). Linear interpolation of the temporal changes in ΔP_t for the Florida region listed in Table 20b of Ho et al. (1987) yields $\Delta P_t \sim 82$ mb at $t = 3.2$ h, which corresponds to a P_t of $\sim$931 mb. Substituting $\Delta P_t = 82$ mb into (11) yields an FR of 0.90. Thus, the filling rates computed for Andrew based on the results of Ho et al. (1987) are too small to explain the observed rate of decay of Andrew. However, if the changes in ΔP_t computed by Ho et al. (1987) for the Gulf of Mexico region are employed instead of those obtained for Florida, the agreement is much better. Linear interpolation of the temporal changes in ΔP_t obtained for the Gulf of Mexico region by Ho et al. (1987, Table 20a) yields $\Delta P_t \sim 70$ mb ($P_t \sim 943$ mb) at $t = 3.2$ h. Substituting this value into (11) yields an FR of 0.77, which is in much better agreement with the observed FR of 0.68 than the 0.90 value obtained using the Florida decay curves of Ho et al. (1987). This example supports the hypothesis that filling rates of hurricanes making landfall along the Florida coastline are probably not significantly different than those in other regions.

4. Applications

The IWDM can be used in a number of applications. The most obvious use is for operational forecasting of the maximum winds associated with landfalling hurricanes. Given a forecast track, the time of landfall and the distance inland as a function of time can be estimated. The storm intensity at landfall is also required for the forecast. DeMaria and Kaplan (1994) have shown that the average 12-h intensity forecast error for storms over the water is about 7 kt, so a reasonable estimate of the landfall intensity could be obtained for storms that are not too far from land. Given this information, (10) could be used to estimate the storm intensity along the inland part of the forecast track.

As an example of the above application, consider the landfall of Hurricane Andrew (1992) in Louisiana. According to the NHC best track, this storm made landfall approximately 150 km west of New Orleans between 0600 and 1200 UTC 26 August 1992 with an intensity of 115 kt and dissipated just after 0600 on 28 August near the Tennessee–North Carolina border. Figure 7 shows the NHC best track intensities at 6-h intervals and the intensity prediction from the IWDM with and without the correction for distance inland [C in Eq. (10)]. The forecast intensities were calculated every half hour, and the intensity was assumed to be constant (115 kt) from 0600 UTC 26 August ($t = 0$) to the landfall point ($t = 2.5$ h). The rapid decrease in intensity at landfall is due to the application of the reduction factor [R in Eq. (10)]. In this example, the best track storm positions (rather than a forecast track) were used to determine the landfall time (by linear interpolation between the 6-h positions) and the distance to the coast after landfall. This figure shows that the model does a reasonable job of predicting the intensity of Andrew after landfall. The maximum error is about 10 kt at 18 h. When the distance inland correction is included, the model predicts slightly lower intensities than without the correction after 18 h. The average of the intensity errors at the eight best track positions after landfall is about the same with and without the distance inland correction (average error about 7 kt).

Although the IWDM was developed from a sample of the maximum winds of landfalling tropical cyclones, it can also be applied to a wind field to provide a crude estimate of the swath of inland winds. For this application, it is necessary to estimate the two-dimensional surface wind field of a storm just prior to landfall. The IWDM can then be applied to every point of this wind field to provide a wind swath. Detailed real-time analyses of hurricane wind fields are being produced as an experimental product (Burpee et al. 1994) but are not yet operational. In the interim, a parametric model similar to that used in storm surge modeling (Hubbert et al. 1991) can be used to obtain a representative surface wind field prior to landfall. The parametric approach assumes that the wind field is the sum of an azimuthally symmetric vortex and a constant vector that represents the storm motion. With this assumption, the wind speed just prior to landfall can be determined by

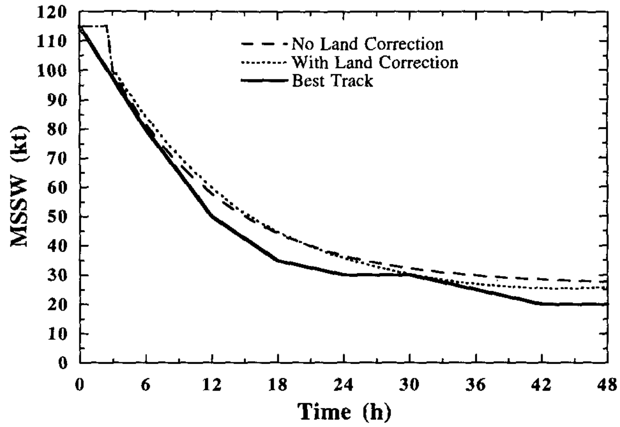

FIG. 7. The observed (6-h interval) and predicted (0.5-h interval) MSSW (kt) for the Louisiana landfall of Hurricane Andrew (1992). The prediction was made with and without the correction for distance inland.

$$V_0(r, \theta) = c_s[\cos(\theta)] + V_x\left(\frac{r}{r_x}\right)\exp\left\{\frac{1}{a}\left[1 - \left(\frac{r}{r_x}\right)^a\right]\right\}. \quad (13)$$

In (13), r is the radial distance from the storm center, and θ is the angle measured counterclockwise from a line perpendicular and to the right of the direction of motion. The wind field in (13) requires the specification of the parameters c_s, V_x, r_x, and a. The parameter c_s is the amplitude of the right to left asymmetry due to the storm motion. The value of this parameter could be determined from an empirical relationship, as a function of the storm translational speed, as described in the appendix. However, as a first approximation, it will be assumed that c_s is equal to the storm translational speed. The parameter V_x is the symmetric part of the MSSW. Because the operational estimate of the MSSW (M_x) of a storm is for the total wind field, V_x is determined by

$$V_x = M_x - c_s. \quad (14)$$

The parameter r_x is the radius of maximum wind. This parameter could be estimated from aircraft data, if available, or from the estimate of the storm-eye diameter that is routinely available on the tropical cyclone forecast/advisory issued by NHC. From an analysis of aircraft observations for several recent landfalling storms, it was found that a crude estimate of r_x can be obtained by taking 0.75 times the eye-diameter estimate. It should also be mentioned, however, that the eye-diameter estimate is not always reliable, especially for weaker storms. The final parameter to be specified is a, which determines the storm size. This parameter can be estimated from aircraft data, if available, or by a least squares fit of (13) to the radii of 65- and 50-kt winds reported on the tropical cyclone forecast/advisory.

Once the wind speed field just prior to landfall is determined, the IWDM model can be applied to every point of this field to estimate the wind field of the storm as it moves inland, where the time in (10) is the time since the storm center made landfall. Because the distance inland calculation is only valid for the storm center, this correction term is neglected when estimating the inland wind field. To provide a wind swath, the maximum wind at any time during the storm can be calculated.

As an example of the above application, consider the landfall of Hurricane Andrew (1992) in south Florida. This case was chosen because a detailed analysis of the maximum wind at any time during the storm has been prepared by Powell and Houston (1995, unpublished manuscript). Their study used all available aircraft and surface observations to produce wind analyses before and after Andrew made landfall in south Florida. According to the NHC best track, the MSSW of Andrew just prior to landfall in south Florida was 125 kt, and the speed of motion was 17 kt. Thus, c_s = 17 kt and V_x = 108 kt. The r_x was set to 17 km, as determined from the wind analysis prior to landfall shown in Powell and Houston (1995, unpublished manuscript). The radius of 50-kt winds in their analysis was used to estimate a, which was set to 0.45 for this case.

Figure 8 shows the observed wind swath and that predicted by the IWDM, where the observed positions were used in the model, rather than a forecast track. The model did a reasonable job of predicting the basic features of the observed wind field, such as the area covered by 35-kt winds and the extent of the inland penetration of the 95-kt wind contour. However, the details of the wind field such as the area covered by 95-kt winds near the landfall point were not well represented. This limitation is probably due to the fact that the simple parametric model cannot capture all of the details of the wind field at landfall, and the IWDM does not well represent the complex interactions that occur as a storm moves over the ocean–land boundary. Fujita (1978) and Wakimoto and Black (1994) provide examples of the complexities of the wind fields associated with landfalling Hurricanes Celia (1970) and Andrew (1992).

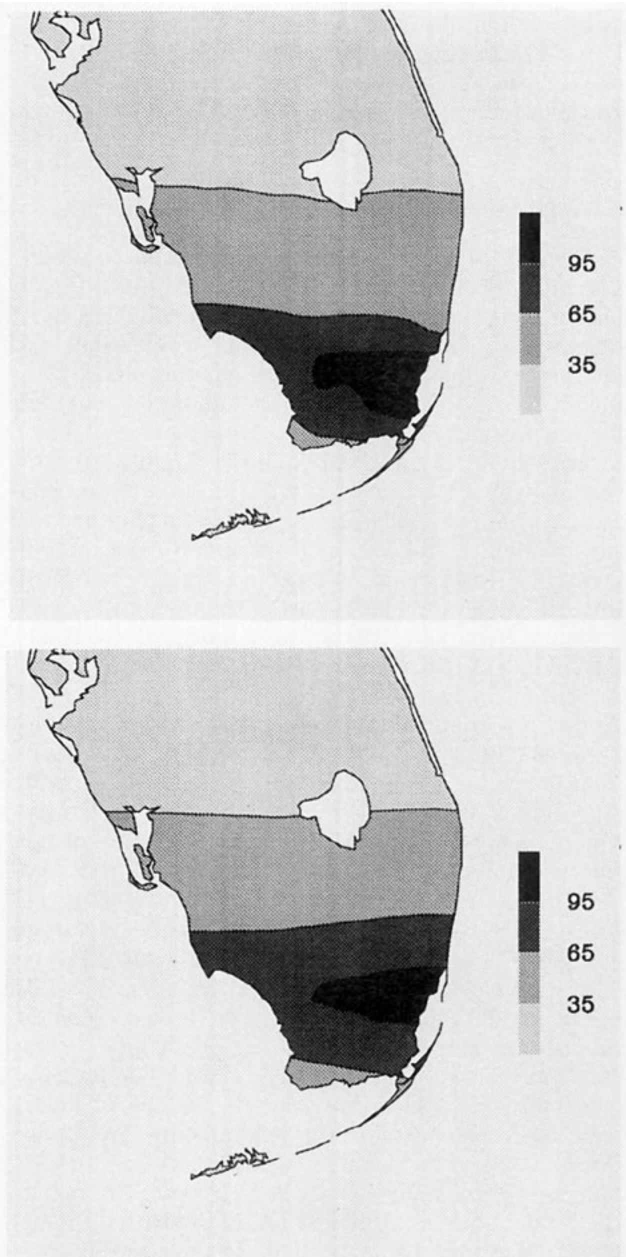

FIG. 8. The observed (top) and predicted (bottom) MSSW (kt) at any time during the south Florida landfall of Hurricane Andrew (1992).

In the above applications, the observed track was used to determine the landfall point and the storm positions over land. In an operational setting, it would be necessary to use a forecast track to run the IWDM. In this case, the uncertainties in the forecast track would probably lead to larger errors than those caused by errors in the IWDM. For example, during the 1993 Atlantic hurricane season, the average error of the official NHC 12-h track forecast was 85 km (Lawrence and Gross 1994). This distance is comparable to the width of the area of hurricane force winds (65 kt) in Fig. 8. If the track used in the IWDM were shifted 85 km to the north or south, there would be almost no overlap between the predicted and observed swaths of hurricane-force winds. One possible solution to this problem is to determine the wind swath for an ensemble of track forecasts. A similar approach is used in storm surge modeling where the maximum envelope of waters (MEOWs) are determined by calculating the maximum level of high water for a set of possible storm tracks in a particular region (Jarvinen and Lawrence 1985).

If the small correction for distance inland is neglected in (10), the inland wind speed depends only on the storm intensity at landfall and the time since landfall. For an inland point, the highest winds will occur from a storm that moves inland perpendicular to the coastline and moves so that the radius of maximum wind passes directly over that point. For a storm moving at a constant speed, the time inland can be determined directly from the shortest distance from that point to the coast. Under these assumptions, maps of the maximum inland penetration of winds can be prepared, given the storm speed of motion and the intensity at landfall.

Figures 9–11 show the maximum possible sustained wind speeds for the Atlantic and Gulf Coasts for hurricanes with a range of landfall intensities and speeds of motion. The speeds of motion (8, 12, and 16 kt) represent slow-, medium-, and fast-moving hurricanes, as determined from the data sample used to develop the IWDM. The slow (fast) speed is the 10th (90th) percentile of the distribution of the hurricane speeds at landfall. The medium speed is the average of the sample. The range of intensities at landfall (75, 105, and 135 kt) represent category 1, 3, and 5 hurricanes. These figures show that all of Florida and a substantial fraction of the other coastal states from Texas to North Carolina are vulnerable to hurricane-force winds, although the probability of occurrence at any given location is, of course, quite low. These figures also show that for inland locations, the effect of the storm speed of motion is just as important as the storm intensity at landfall. For example, hurricane-force winds penetrate farther inland for a fast-moving category 3 storm (Fig. 10) than for a slow-moving category 5 storm (Fig. 11).

The data sample used to develop the IWDM is not long enough to accurately determine the distribution of storm speeds and intensities at landfall. However, by using a longer time period and more sophisticated statistical techniques such as those described by Darling (1991), the speed and intensity distributions could be determined. These distributions could then be combined with the IWDM to estimate the probability of hurricane force and other wind thresholds at inland locations.

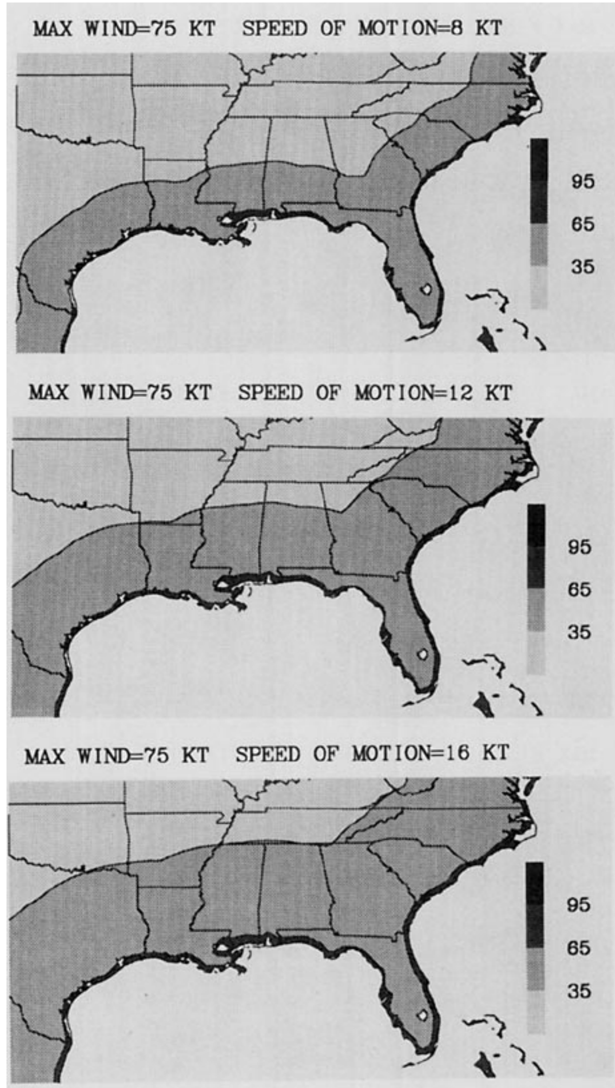

FIG. 9. The maximum possible sustained inland wind speed (kt) for any slow- (top), medium- (middle), or fast- (bottom) moving category 1 (75 kt at landfall) storm.

5. Summary and conclusions

An empirical model for predicting the decay of TC winds after landfall [referred to as the Inland Wind Decay Model (IWDM)] has been described. The IWDM is a simple two-parameter model that was derived based upon the assumption that TC winds decay exponentially with time after landfall. The database used to derive the model consisted of all named TCs that made landfall in the United States south of 37°N between 1967 and 1993. Three hurricanes that made landfall along the Florida coastline prior to 1967 were also included in the sample. Position and intensity estimates for these landfalling storms were obtained from the NHC HURDAT file, except for the intensity estimates for the Florida hurricanes that were derived

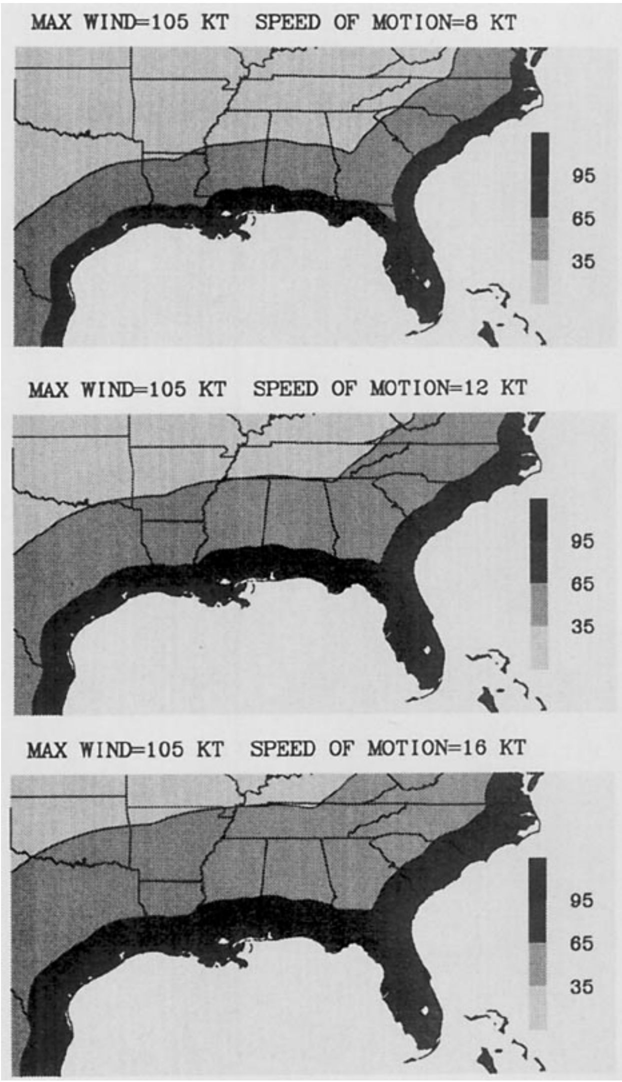

based upon data obtained from the NCDC and the U.S. Army Corps of Engineers.

This study shows that the basic version of the IWDM explains 91% of the variance of the decay of the MSSW for the 401 cases in the developmental database. When an additional term is included in the model to account for the mean distance inland of a TC during the forecast period, the variance explained increased to 93%. This term was added because several studies have shown that TCs that move parallel to the coastline decay less rapidly than TCs that move directly inland. The results of this study also suggest that there do not appear to be significant regional variations in the decay rates of landfalling TCs, in contrast to results from previous studies. It is possible that some minor regional differences in decay rates exist, but cannot be detected because of the limited accuracy of the wind speed estimates used to develop the IWDM. Further investigation of the regional differences in the decay rates of TCs is warranted.

Several applications of the IWDM were described. The IWDM can predict the maximum sustained surface winds as a function of time after landfall, as well as provide a swath of wind speeds produced by landfalling TCs. To provide the wind swath, the IWDM is applied to the tropical cyclone wind field at landfall. Perhaps most importantly, the IWDM can produce maps of the maximum possible sustained surface wind speeds that inland locations would experience for TCs of various landfall intensities and speeds of forward motion. These maps demonstrate that the speed of forward motion of a landfalling TC is just as important as the landfall intensity when assessing how far inland strong winds will penetrate.

Further research is required to refine the IWDM. Observational studies of the decay of TC winds over

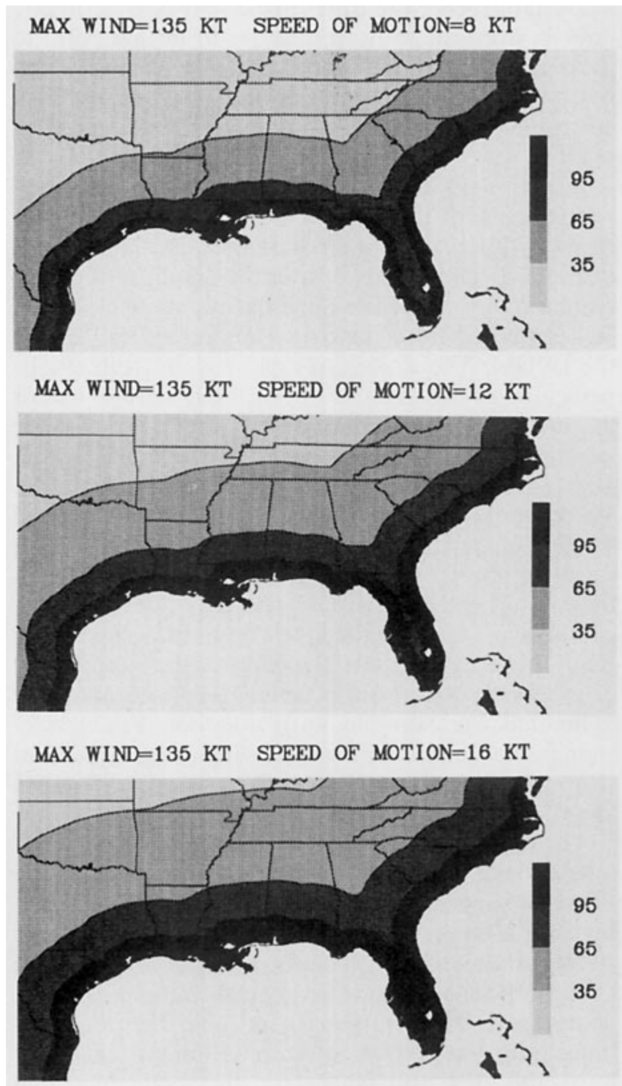

FIG. 11. Same as Fig. 9 for a category 5 (135 kt at landfall) storm.

land would be particularly useful for verifying the model, especially for the case where the entire wind field is predicted. Moreover, the IWDM could be improved by employing a boundary layer model to predict the wind direction as well as wind speed. Finally, a model similar to the IWDM described in this study could be developed for the New England region. These high-latitude storms were eliminated from the present study because topography and interaction with baroclinic weather systems might have significant effects on storm decay in this area.

Acknowledgments. We wish to thank Drs. R. B. Burpee and M. D. Powell, and S. H. Houston of HRD for their constructive reviews of an earlier version of this paper. The authors benefited from the helpful suggestions of Dr. M. D. Powell during the course of this research. Tom Ross of NCDC supplied the data for Hurricanes Donna (1960) and Cleo (1964), and Mark Powell and Sam Houston provided the wind fields that were used to develop the parametric wind model described in section 4. Dr. Robert Merrill of the Cooperative Institute for Meteorological Studies in Madison, Wisconsin, provided much of the computer code used to determine a storm's distance from the coastline, and Mike Black of HRD assisted with the preparation of several of the figures. This research was partially funded by the Federal Emergency Management Agency (FEMA).

APPENDIX

Estimating the MSSWs of Pre-1967 Landfalling Florida Hurricanes

Surface data archived at the National Climatic Data Center (NCDC) were used to obtain position and intensity estimates for Hurricanes Donna (1960) and Cleo (1964). The wind data employed to obtain intensity estimates for the unnamed 1949 Florida hurricane were obtained from a report by the U.S. Weather Bureau (1951). The NCDC data for Hurricanes Cleo and Donna consisted of hard copies of daily observation logs that contained wind direction, sustained wind speed, wind gusts, surface pressures, and other information typically found in surface aviation weather observations. Although the time resolution of the observations varied, the resolution of the wind observations was normally several minutes when a TC was closest to the particular observing site. The daily observation logs contained other important information, such as the magnitude and time of the maximum sustained wind and/or wind gust, the minimum surface pressure, and the timing of any observed eye passage. The wind data obtained from the U.S. Weather Bureau consisted of a series of sustained 10-min winds and surface pressures recorded within a few hours of the time of eye passage of the unnamed 1949 hurricane over Lake Okeechobee. These observations were obtained from a special observing array on Lake Okeechobee that was set up by the U.S. Army Corps of Engineers.

The tracks for the three additional Florida storms were obtained from the HURDAT file. Although the storm positions before 1967 are thought to be somewhat less accurate than those in succeeding years as described previously, the HURDAT tracks for these three storms are in good agreement with those presented in the detailed studies and meteorological accounts given in the U.S. Weather Bureau (1951), Miller (1964), and Dunn (1965). The storm positions are also consistent with the timing of the maximum wind observed for each of these storms. An observation was judged to be close enough to the storm center for the purpose of determining the MSSW if the observing site was at a distance comparable to the radius of maximum wind The radius of maximum wind values for these storms was obtained from Ho et al. (1987). Based on this criterion, a combined total of six observations for the three storms was close enough to the storm center to be used to estimate the MSSW at a specific time after landfall.

Because the above wind observations were representative of various anemometer heights and averaging times, it was necessary to standardize these observations to obtain winds consistent with those in the HURDAT file (i.e., the MSSW). The research of Powell et al. (1991, 1995, unpublished manuscript) has shown the importance of employing such standardization techniques when analyzing landfalling hurricanes. The first step in this process was to adjust the winds to the 10-m level using a neutral stability log wind law (Panofsky and Dutton 1984). The anemometer heights of the observing sites were obtained from the *National Wind Data Index* (Changery 1978). Unfortunately, the index does not provide a direct means of estimating the site roughness length required for use in the log wind law calculations. However, because nearly all of the sites were located at airports, a roughness length corresponding to open airport exposure (Panofsky and Dutton 1984) was assumed when adjusting winds to 10 m. Since the observations represented winds averaged over various time periods, gust factor relationships developed by Powell et al. (1995, unpublished manuscript) were used to convert these winds to 1-min average values. They developed these relationships based on the work of Durst (1960), Krayer and Marshal (1992), and from National Oceanic and Atmospheric Administration moored buoy data collected by the National Data Buoy Center and analyzed by the Hurricane Research Division of the Atlantic Oceanographic and Meteorological Laboratory since 1979. An asymmetry factor developed by Schwerdt et al. (1979) was then added to these wind speeds to obtain estimates of the storm's MSSW. This was done since the wind observations were rarely located in the right front quadrant of the TC where the strongest winds are typically observed (Shea and Gray 1973; Frank 1977). The asymmetry factor was formulated such that a fraction of the storm speed of forward motion is added to winds on the right side of the TC and subtracted from winds on the left side. The relationship itself is somewhat conservative since the asymmetry factor is always less than the storm speed of motion. The average change in wind speed resulting from the above standardization procedures was about 20%.

REFERENCES

Batts, M. E., M. R. Cordes, L. R. Russell, J. R. Shaver, and E. Simiu, 1980: Hurricane wind speeds in the United States. National Bureau of Standards Building Science Series 124, U.S. Department of Commerce, 50 pp.

Bender, M. A., R. J. Ross, R. E. Tuleya, and Y. Kurihara, 1993: Improvements in tropical cyclone track and intensity forecasts using the GFDL initialization system. *Mon. Wea. Rev.,* **121,** 2046–2061.

Burpee, R. W., and Coauthors, 1994: Real-time guidance provided by NOAA's Hurricane Research Division to forecasters during Emily of 1993. *Bull. Amer. Meteor. Soc.,* **75,** 1765–1783.

Changery, M. J., 1978: *National Wind Data Index Final Report.* U.S. Department of Commerce, 245 pp.

Darling, R. W. R., 1991: Estimating probabilities of hurricane wind speeds using a large-scale empirical model. *J. Climate,* **4,** 1035–1046.

DeMaria, M., and J. Kaplan, 1994: A statistical hurricane intensity prediction scheme (SHIPS) for the Atlantic basin. *Wea. Forecasting,* **9,** 209–220.

Dunn, G. E., and Staff, 1965: The hurricane season of 1964. *Mon. Wea. Rev.,* **93,** 175–187.

Durst, C. S., 1960: Wind speeds over short periods of time. *Meteor. Mag.,* **89,** 181–186.

Frank, W. M., 1977: The structure and energetics of the tropical cyclone. Part I: Storm structure. *Mon. Wea. Rev.,* **105,** 1119–1135.

Fujita, T. T., 1978: Manual of downburst identification for Project NIMROD. SMRP Res. Paper 156, University of Chicago, 104 pp.

Georgiou, P. N., 1985: Design wind speeds in tropical cyclone-prone regions. Ph.D. dissertation, University of Western Ontario, 295 pp.

Ho, F. P., J. C. Su, K. L. Hanevich, R. J. Smith, and F. P. Richards, 1987: Hurricane climatology for the Atlantic and Gulf Coasts of the United States. NOAA Tech. Rep. NWS 38, 195 pp. [Available from NWS/NOAA, U.S. Dept. of Commerce, 8060 13th St., Silver Spring, MD 20910.]

Hubbert, G. D., G. J. Holland, L. M. Leslie, and M. J. Manton, 1991: A real-time system for forecasting tropical cyclone storm surges. *Wea. Forecasting,* **6,** 86–97.

Hubert, L. F., 1955: Frictional filling of hurricanes. *Bull. Amer. Meteor. Soc.,* **36,** 440–445.

Jarvinen, B. R., and M. B. Lawrence, 1985: An evaluation of the SLOSH storm surge model. *Bull. Amer. Meteor. Soc.,* **66,** 1408–1411.

——, C. J. Neumann, and M. A. S. Davis, 1988: A tropical cyclone data tape for the North Atlantic Basin, 1886–1983: Contents, limitations, and uses. NOAA Tech. Memo. NWS NHC 22, Miami, FL, 21 pp.

Jorgensen, D. P., 1984: Mesoscale and convective-scale characteristics of mature hurricanes. Part I: General observations by research aircraft. *J. Atmos. Sci.,* **41,** 1268–1285.

Krayer, W. R., and R. D. Marshal, 1992: Gust factors applied to hurricane winds. *Bull. Amer. Meteor. Soc.,* **73,** 613–617.

Lawrence, M. B., 1994: 1993 National Hurricane Center forecast verification. *Minutes of the 48th Interdepartmental Conf.,* Miami, FL, Office of Fed. Coord. for Meteor. Services and Supporting Research, NOAA, B-15–B-24.

——, and J. M. Gross, 1993: 1992 National Hurricane Center forecast verification. *Minutes of the 47th Interdepartmental Conf.,* Miami, FL, Office of Fed. Coord. for Meteor. Services and Supporting Research, NOAA, B-13–B-21.

Malkin, W., 1959: Filling and intensity changes in hurricanes over land. National Hurricane Research Project Rep. 34. U.S. Weather Bureau, Washington, DC, 18 pp.

Mayfield, M., M. L. Avila, and E. N. Rappaport, 1994: Atlantic hurricane season of 1992. *Mon. Wea. Rev.,* **122,** 517–538.

Merrill, R. T., 1987: An experiment in statistical prediction of tropical cyclone intensity change. NOAA Tech. Memo. NWS NHC-34, 34 pp.

Miller, B. I., 1964: A study on the filling of Hurricane Donna (1960) over land. *Mon. Wea. Rev.,* **92,** 389–406.

Myers, V. A., 1954: Characteristics of United States hurricanes pertinent to levee design for Lake Okeechobee, FL. Hydrometeorological Rep. 32. U.S. Department of Commerce, Washington, DC, 106 pp.

National Research Council, 1994: *Hurricane Hugo: Puerto Rico, The U.S. Virgin Islands, and South Carolina September 17–22, 1989.* National Academy Press, 276 pp.

Neumann, C. J., 1994: An update to the National Hurricane Center "Track Book." *Minutes of the 48th Interdepartmental Conf.,* Miami, FL, Office of Fed. Coord. for Meteor. Services and Supporting Research, NOAA, A-47–A-53.

Ooyama, K., 1969: Numerical simulation of the life cycle of tropical cyclones. *J. Atmos. Sci.,* **26,** 3–40.

Panofsky, H. A., and J. A. Dutton, 1984: *Atmospheric Turbulence.* Wiley-Interscience. 397 pp.

Powell, M. D., 1982: The transition of the Hurricane Frederic boundary layer wind fields from the open Gulf of Mexico to landfall. *Mon. Wea. Rev.,* **110,** 1912–1932.

——, 1987: Changes in the low-level kinematic and thermodynamic structure of Hurricane Alicia (1983) at landfall. *Mon. Wea. Rev.,* **115,** 75–99.

——, P. P. Dodge, and M. L. Black, 1991: The landfall of Hurricane Hugo in the Carolinas: Surface wind distribution. *Wea. Forecasting,* **6,** 379–399.

Rosenthal, S. L., 1971: The response of a tropical cyclone model to variations in boundary layer parameters, initial conditions, lateral boundary conditions, and domain size. *Mon. Wea. Rev.,* **99,** 767–777.

Samsury, C. E., and E. J. Zipser, 1995: Secondary wind maxima in hurricanes: Airflow and relationship to rainbands. *Mon. Wea. Rev.,* in press.

Schwerdt, R. W., F. P. Ho, and R. R. Watkins, 1979: Meteorological criteria for standard project hurricane and probable maximum hurricane windfields, Gulf and East Coasts of the United States, NOAA Tech. Rep. NWS 23, 317 pp. [Available from NWS NOAA, U.S. Department of Commerce, 8060 13th St. Silver Spring, MD 20910.]

Shapiro, L. J., 1983: The asymmetric boundary layer flow under a translating hurricane. *J. Atmos. Sci.,* **40,** 1984–1998.

Shea, D. J., and W. M. Gray, 1973: The hurricane's inner core region. Part I: Symmetric and asymmetric structure. *J. Atmos. Sci.,* **30,** 1544–1563.

Tuleya, R. E., 1994: Tropical storm development and decay: Sensitivity to surface boundary conditions. *Mon. Wea. Rev.,* **122,** 291–304.

——, M. A. Bender, and Y. Kurihara, 1984: A simulation study of the landfall of tropical cyclones using a movable nested-mesh model. *Mon. Wea. Rev.,* **112,** 124–136.

U.S. Department of Commerce, 1993: *Hurricane Andrew: South Florida and Louisiana August 23–26, 1992.* U.S. Department of Commerce, 131 pp.

U.S. Weather Bureau, 1951: Analysis of winds over Lake Okeechobee during tropical storm of August 26–27, 1949. Hydrometeorological Rep. 26., U.S. Department of Commerce, Washington, DC, 80 pp.

Wakimoto, R. M., and P. G. Black, 1994: Damage survey of Hurricane Andrew and its relationship to the eyewall. *Bull. Amer. Meteor. Soc.,* **75,** 189–200.